

Effect of spin-orbit coupling on the excitation spectrum of Andreev billiards

B. Béri,¹ J. H. Bardarson,² and C. W. J. Beenakker²

¹*Department of Physics of Complex Systems, Eötvös University,
H-1117 Budapest, Pázmány Péter sétány 1/A, Hungary*

²*Instituut-Lorentz, Universiteit Leiden, P.O. Box 9506, 2300 RA Leiden, The Netherlands*

(Dated: December, 2006)

We consider the effect of spin-orbit coupling on the low energy excitation spectrum of an Andreev billiard (a quantum dot weakly coupled to a superconductor), using a dynamical numerical model (the spin Andreev map). Three effects of spin-orbit coupling are obtained in our simulations: In zero magnetic field: (1) the narrowing of the distribution of the excitation gap; (2) the appearance of oscillations in the average density of states. In strong magnetic field: (3) the appearance of a peak in the average density of states at zero energy. All three effects have been predicted by random-matrix theory.

PACS numbers: 74.45.+c, 71.70.Ej, 05.45.Pq, 74.78.Na

I. INTRODUCTION

A quantum dot in a two-dimensional electron gas has a mean level spacing which is independent of energy and depends only on geometrical factors (area) and material properties (effective mass). The nature of the electron dynamics (chaotic versus integrable) and the presence or absence of symmetries, such as time-reversal and spin-rotation symmetry, have no effect on the mean density of states. The situation changes if the quantum dot is coupled to a superconductor (see Fig. 1). The presence of the superconductor strongly affects the excitation spectrum of such an Andreev billiard. The density of states at the Fermi level is suppressed in a way which is sensitive to the nature of the dynamics and existing symmetries.¹ While the effect of broken time-reversal symmetry on the density of states has been studied extensively,^{2,3,4,5} the effect of broken spin-rotation symmetry due to spin-orbit coupling has only been partially investigated.^{6,7,8}

In this paper we study in computer simulations three effects of the spin-orbit coupling. All of these effects have been predicted by random-matrix theory (RMT),^{6,9,10} but have so far not been confirmed in a dynamical model. The first two of these effects,^{9,10} present in the absence

of a magnetic field, are the reduction of the sample-to-sample fluctuations of the excitation gap and the appearance of oscillations as a function of energy in the average density of states. The third effect appears in a magnetic field strong enough to close the excitation gap. While in the absence of spin-orbit coupling the average density of states vanishes at the Fermi level, in the presence of spin-orbit coupling it peaks at the Fermi level at twice the value in the normal state.⁶

II. PREDICTIONS OF RANDOM-MATRIX THEORY

We begin by briefly summarizing the RMT of the Andreev billiard.¹ In perturbation theory the density of states of non-degenerate levels (in zero or weak magnetic field) has a square root dependence on energy near the gap,^{4,11}

$$\rho_{\text{pert}}(E) = \frac{1}{\pi} \sqrt{\frac{E - E_{\text{gap}}}{\Delta_{\text{gap}}^3}}, \quad E \rightarrow E_{\text{gap}}. \quad (1)$$

The parameters E_{gap} and Δ_{gap} are given by

$$E_{\text{gap}} = cE_T, \quad \Delta_{\text{gap}} = \left(\frac{s\delta}{2}\right)^{2/3} \left(\frac{dE_T}{4\pi^2}\right)^{1/3}. \quad (2)$$

Here $\delta = 2\pi\hbar^2/mA$ is the mean level spacing in the isolated quantum dot (area A , effective mass m), $N = \text{Int}[k_F W/\pi]$ is the number of modes in the ballistic point contact (width W , Fermi wave vector k_F) connecting it to the superconductor, and $E_T = N\delta/4\pi$ is the Thouless energy. These parameters refer to two-fold degenerate levels and modes, corresponding to $s = 2$. If both spin-rotation and time-reversal symmetries are broken, the two-fold degeneracy is lifted and one should take $s = 1$. The numerical coefficients c and d are magnetic field dependent. For $B = 0$ one has

$$c = 2\gamma^{5/2}, \quad d = (5 - 2\sqrt{5})\gamma^{5/2}, \quad (3)$$

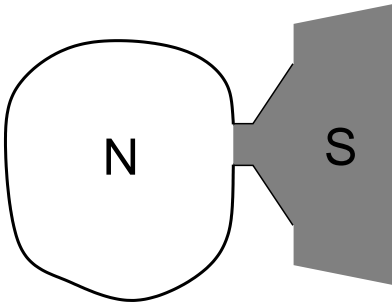


Figure 1: Sketch of an Andreev Billiard: A quantum dot (N) connected to a superconductor (S) by a point contact. Spin-orbit coupling is present in the quantum dot.

with $\gamma = (\sqrt{5} - 1)/2$ the reciprocal of the golden ratio. For $B \neq 0$ they should be calculated from the RMT solution given in Ref. 4.

The perturbation theory has δ/E_T as a small parameter and gives the density of states with an energy resolution of order E_T , which is a macroscopic energy scale. Since spin-orbit effects typically appear as quantum corrections, no sign of spin-orbit coupling can be seen in such a calculation. In particular, the magnetic field dependence of the perturbative density of states is the same with and without spin-orbit coupling — the only difference being that in a magnetic field, in the absence of spin-rotation symmetry, there is no level degeneracy thus Δ_{gap} is $2^{2/3}$ times smaller than in the spin-rotation symmetric case.

To capture the spectral properties on the mesoscopic energy scale of order Δ_{gap} , one needs to go beyond perturbation theory. According to the universality hypothesis of Vavilov *et al.*¹⁰ the probability distribution of the lowest level E_1 in properly scaled units is universal and identical to the distribution of the smallest eigenvalue of random Gaussian matrices from the three symmetry classes of RMT. The appropriate scaling is in terms of the dimensionless variable $x_1 = (E_1 - E_{\text{gap}})/\Delta_{\text{gap}}$ and the universal distributions are given by^{9,12}

$$P_\beta(x_1) = -\frac{d}{dx_1} F_\beta(x_1), \quad (4)$$

where

$$F_1(x) = \sqrt{F_2(x)} \exp\left(-\frac{1}{2} \int_{-\infty}^x q(x') dx'\right), \quad (5a)$$

$$F_2(x) = \exp\left(-\int_{-\infty}^x (x-x')q(x')^2 dx'\right), \quad (5b)$$

$$F_4\left(\frac{x}{2^{2/3}}\right) = \sqrt{F_2(x)} \cosh\left(\frac{1}{2} \int_{-\infty}^x q(x') dx'\right). \quad (5c)$$

The function $q(x)$ is the solution of the differential equation

$$q''(x) = -xq(x) + 2q^3(x).$$

The boundary condition is $q(x) \rightarrow \text{Ai}(-x)$ as $x \rightarrow -\infty$, with $\text{Ai}(x)$ being the Airy function. The three distributions are plotted in Fig. 2 (top panel). The symmetry index β takes values $\beta = 1$ for time-reversal and spin-rotation invariant systems, $\beta = 4$ when time-reversal symmetry is present but spin-rotation symmetry is broken, and $\beta = 2$ for systems with broken time-reversal symmetry.

Near the gap, the average density of states in terms of the variable $x = (E - E_{\text{gap}})/\Delta_{\text{gap}}$ is given by^{13,14}

$$\rho_1(x) = \rho_2(x) + \frac{1}{2} \text{Ai}(-x) \left[1 - \int_{-x}^{\infty} \text{Ai}(y) dy\right], \quad (6a)$$

$$\rho_2(x) = x \text{Ai}^2(-x) + [\text{Ai}'(-x)]^2, \quad (6b)$$

$$2^{1/3} \rho_4\left(\frac{x}{2^{2/3}}\right) = \rho_2(x) - \frac{1}{2} \text{Ai}(-x) \int_{-x}^{\infty} \text{Ai}(y) dy. \quad (6c)$$

The distribution P_2 and the density of states ρ_2 are applicable in an intermediate magnetic field range, which exists because the flux needed to close the gap is much larger than the flux needed to break the time-reversal symmetry. For intermediate fluxes ($\Phi \gtrsim (h/e)N^{1/3} \sqrt{\tau_{\text{erg}}\delta/\hbar}$ with $\tau_{\text{erg}} = \sqrt{A}/v_F$ the ergodic time and v_F the Fermi velocity), there will still be a gap, but its fluctuations are governed by the $\beta = 2$ symmetry class. In this case the presence or absence of spin-orbit coupling only affects the parameter Δ_{gap} (which is reduced by a factor $2^{2/3}$ in the absence of spin-orbit coupling, because the level degeneracy parameter goes from $s = 2$ to $s = 1$); the gap distribution P_2 and the density of states ρ_2 in rescaled variables do not depend on the presence or absence of spin-rotation symmetry.

If the flux is made much larger ($\Phi \gg (h/e)\sqrt{N\tau_{\text{erg}}\delta/\hbar}$), such that the gap closes, spin-orbit coupling starts to play a role again. The reason is that an energy level E and its mirror level at $-E$ can repel each other, and this repulsion depends on the presence or absence of spin-orbit coupling. When there is still a gap these levels are widely separated and this repulsion is not effective.⁶

According to Altland and Zirnbauer,⁶ the RMT of an Andreev billiard in strong magnetic field is in a new symmetry class called C (D) in the absence (presence) of spin-orbit coupling. The average density of states in these symmetry classes is

$$\rho_{\pm}(E) = \frac{4}{s\delta} \left[1 \pm \frac{\sin(8\pi E/s\delta)}{8\pi E/s\delta}\right]. \quad (7)$$

The minus (plus) sign should be taken for symmetry class C (D). This result expresses the fact that in the absence of spin-orbit coupling, a level and its mirror level repel each other leading to a vanishing density of states at $E = 0$. In the presence of spin-orbit coupling the repulsion disappears and levels pile up at the Fermi level, leading to a peak in the density of states at $E = 0$.

III. SPIN ANDREEV MAP

To verify these predictions of RMT in a dynamical model we combine the general construction of an Andreev map¹⁵ with the spin kicked rotator.^{16,17} The starting point of our discussion is the spin generalized Bogoliubov-De Gennes Hamiltonian¹⁸

$$\mathcal{H}_{\text{BdG}} = \begin{pmatrix} H - E_F & \Delta \\ \Delta^* & E_F - \mathcal{T}H\mathcal{T}^{-1} \end{pmatrix}. \quad (8)$$

Here H is the single particle Hamiltonian, E_F is the Fermi energy, and Δ is the superconducting pair-potential. The operator \mathcal{T} stands for time-reversal, and will be specified later.

With the Bogoliubov-De Gennes Hamiltonian as a guide we construct the spin Andreev map. First we note that if an electron in the normal metal evolves with

time-evolution operator $F(t)$, the hole evolves with the transformed time-evolution operator $\mathcal{T}F(t)\mathcal{T}^{-1}$. Second, since we are interested in low energy phenomena, only the dynamics on long time scales is important. On time scales much larger than τ_{erg} , the dynamics can be described as a mapping on a two-dimensional Poincaré surface of section. This amounts to a stroboscopic description where we are only concerned with the state of the electron when it bounces off the boundary.

The quantum map we use is the computationally efficient spin kicked rotator, given in terms of a Floquet matrix,^{16,17}

$$F_{ll'} = e^{i\varepsilon_0} (\Pi U X U^\dagger \Pi)_{ll'}, \quad l, l' = 0, 1, \dots, M-1. \quad (9)$$

The integer M sets the level spacing $\delta = 2\pi/M$. The $M \times M$ matrices appearing in Eq. (9) have quaternion matrix elements, and are given by

$$\Pi_{ll'} = \delta_{ll'} e^{-i\pi(l+l_0)^2/M} \sigma_0, \quad (10a)$$

$$U_{ll'} = M^{-1/2} e^{-i2\pi ll'/M} \sigma_0, \quad (10b)$$

$$X_{ll'} = \delta_{ll'} e^{-i(M/4\pi)V(2\pi l/M)}, \quad (10c)$$

with

$$V(\theta) = K \cos(\theta + \theta_0) \sigma_0 + K_{\text{so}}(\sigma_1 \sin 2\theta + \sigma_3 \sin \theta). \quad (11)$$

The quaternions are represented using the Pauli matrices σ_i with σ_0 the 2×2 unit matrix. The matrix X corresponds to the spin-orbit coupled free motion inside the dot and Π gives scattering off the boundaries of the dot. This map is classically chaotic for kicking strength $K \gtrsim 7.5$. The parameter K_{so} breaks spin-rotation symmetry, θ_0 breaks time-reversal symmetry and l_0 breaks other symmetries of the map. The spin-orbit coupling time τ_{so} (in units of the stroboscopic period $\tau_0 \approx \tau_{\text{erg}}$) is related to K_{so} through $\tau_{\text{so}} = 32\pi^2/(K_{\text{so}}M)^2$. The parameter ε_0 corresponds to the Fermi energy. In the above representation of the Floquet matrix, the time-reversal operator is given by $\mathcal{T} = i\sigma_2\mathcal{K}$ where \mathcal{K} is the operator of complex conjugation.¹⁷ Therefore, the hole Floquet matrix is given by $\sigma_2 F^* \sigma_2 \equiv \bar{F}$, where the overbar denotes quaternionic complex conjugation.

The spin Andreev map is constructed from the electron and hole Floquet matrices in the same way as in the absence of spin-orbit coupling,¹⁵

$$\mathcal{F} = \mathcal{P} \begin{pmatrix} F & 0 \\ 0 & \bar{F} \end{pmatrix}, \quad (12a)$$

$$\mathcal{P} = \begin{pmatrix} 1 - P^T P & -iP^T P \\ -iP^T P & 1 - P^T P \end{pmatrix}. \quad (12b)$$

The projection matrix P projects onto the contact with the superconductor. Its matrix elements are $P_{kl} = \delta_{kl}\sigma_0 \sum_{i=1}^N \delta_{l,n_i}$ where the set of indices $\{n_i\}$ corresponds to the modes coupled to the superconductor. The dwell time is therefore $\tau_{\text{dwell}} = M/N$. The corresponding Thouless energy is $E_T = N\delta/4\pi = (2\tau_{\text{dwell}})^{-1}$. As shown

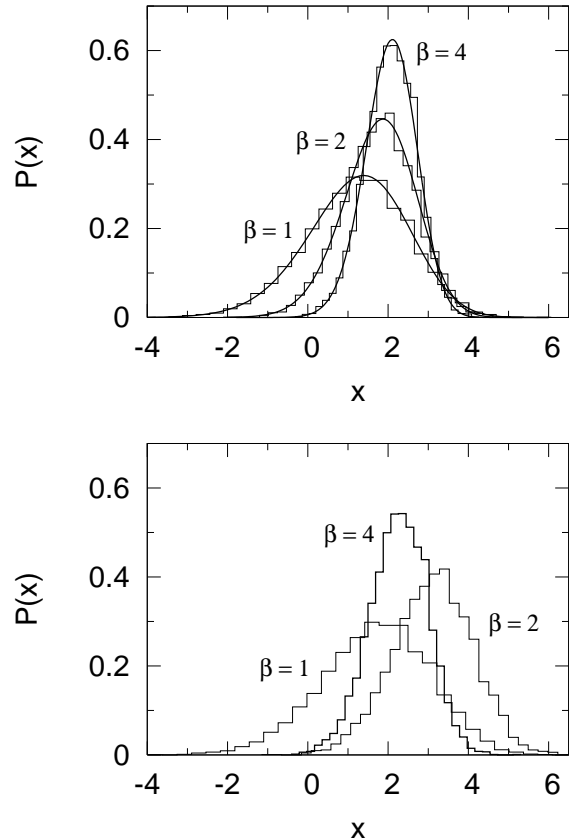


Figure 2: Probability distribution of the rescaled excitation gap $x = (E_1 - E_{\text{gap}})/\Delta_{\text{gap}}$. Smooth curves (upper panel) are the predictions of random-matrix theory, for the three symmetry classes $\beta = 1, 2, 4$. Histograms are the results of the numerical simulation of the spin Andreev map, without spin-orbit coupling (zero magnetic field, $\beta = 1$) and with spin-orbit coupling (zero magnetic field, $\beta = 4$; weak magnetic field, $\beta = 2$). The histograms in the lower panel are plotted without any fitting, while in the upper panel E_{gap} and Δ_{gap} are treated as fit parameters.

in Ref. 17, the magnetic field scale at which the gap closes is given by $\theta_c = 4\pi\sqrt{N}/(KM^{3/2})$. From the definitions in Eq. (2) the scaling parameters in the spin Andreev map become

$$E_{\text{gap}} = \frac{cN}{2M}, \quad \Delta_{\text{gap}} = \frac{(s^2 dN)^{1/3}}{2M}. \quad (13)$$

The Floquet matrix has the symmetry

$$\mathcal{F} = \mathcal{C}\mathcal{T}\mathcal{F}(\mathcal{C}\mathcal{T})^{-1}, \quad \mathcal{C} = \begin{pmatrix} 0 & -1 \\ 1 & 0 \end{pmatrix}, \quad (14)$$

corresponding to the $\mathcal{C}\mathcal{T}$ -antisymmetry of \mathcal{H}_{BdG} , the fundamental discrete symmetry of normal-superconducting systems.⁶ The eigenphases of the Floquet matrix \mathcal{F} , defined as the solutions of

$$\det(\mathcal{F} - e^{-i\varepsilon}) = 0, \quad (15)$$

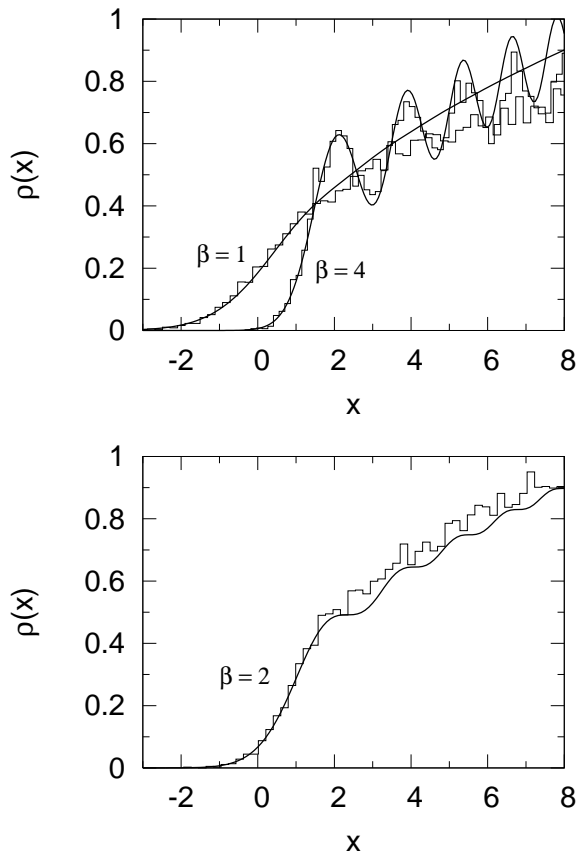


Figure 3: Average density of states in rescaled energy units, $x = (E - E_{\text{gap}})/\Delta_{\text{gap}}$, in zero magnetic field (upper panel, $\beta = 1, 4$) and in a weak magnetic field (lower panel, $\beta = 2$). The smooth curves are the RMT predictions, the histograms are the results of the simulation (using the same values of the fit parameters $E_{\text{gap}}, \Delta_{\text{gap}}$ as in the upper panel of Fig. 2).

play the role of the discrete excitation energies in the Andreev billiard. From the symmetry (14) it follows that they come in pairs, $\pm\varepsilon$, as required.

IV. NUMERICAL RESULTS AND COMPARISON WITH RMT

In Fig. 2 we plot the excitation gap distribution (histograms) from our numerical simulation with parameters $K = 41.123$, $M = 4096$, $N = 205$. The smallest ε solving Eq. (15) was calculated for some 6000 different Fermi energies and positions of the contact to the superconductor. To generate the three symmetry classes we took: $\theta_0/\theta_c = 0$, $\tau_{\text{dwell}}/\tau_{\text{so}} = 0$ ($\beta = 1$); $\theta_0/\theta_c = 0$, $\tau_{\text{dwell}}/\tau_{\text{so}} = 625$ ($\beta = 4$); $\theta_0/\theta_c = 0.4$, $\tau_{\text{dwell}}/\tau_{\text{so}} = 625$ ($\beta = 2$). The values of the parameters c and d for $\theta_0/\theta_c = 0$ are given by Eq. (3). For $\theta_0/\theta_c = 0.4$ we calculate $c = 0.427$, $d = 0.339$ from Ref. 4. The data is shown without any fit parameter in the lower panel and with

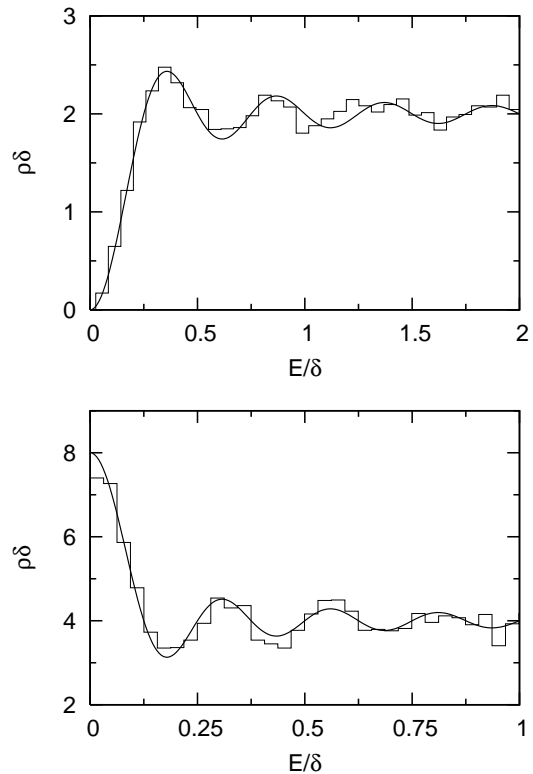


Figure 4: Average density of states in a magnetic field sufficiently strong to close the excitation gap. Upper panel: without spin-orbit coupling; Lower panel: with spin-orbit coupling. The smooth curves are the RMT predictions from Eq. (7) and the histograms are the results of the simulation (now without any fit parameters).

$E_{\text{gap}}, \Delta_{\text{gap}}$ as fit parameters in the upper panel. (A similar fitting procedure was used in Ref. 19.) The fitted values of E_{gap} and Δ_{gap} do not vary much (by about 5% and 10%, respectively) from their nominal values [given by Eq. (13)], but the agreement with the RMT predictions improves considerably if we allow for this variation.²⁰

The characteristics of the gap distribution are clearly obtained in our simulation. In zero magnetic field, the gap distribution becomes narrower as the strength of spin-orbit coupling is increased ($\beta = 1 \rightarrow 4$). The RMT prediction for the standard deviation of the scaled distributions $P_\beta(x)$ is $\sigma_1 = 1.27$ and $\sigma_4 = 0.64$. The corresponding values obtained in our numerical simulation *without any fitting* are $\sigma_1 = 1.34$ and $\sigma_4 = 0.72$. If a weak magnetic field is present ($\beta = 2$), the width of the distribution is predicted to be intermediate between the cases with $\beta = 1, 4$. As seen, the dynamical model follows the prediction. The theoretical value of the standard deviation is $\sigma_2 = 0.90$, the numerical result (without fitting) is $\sigma_2 = 0.99$.

Using the same fit parameters as in Fig. 2 we plot the average density of states close to the gap in Fig. 3. As seen, the numerical data follow closely the analytical pre-

dictions, the deviations becoming significant only outside the universal regime $|E - E_{\text{gap}}| \ll E_T$, i.e. $|x| \ll N^{2/3}$. In the absence of magnetic field the spin-orbit coupling induced oscillations are clearly obtained.

The density of states in a strong magnetic field is given in Fig. 4. The upper panel shows the data without spin-orbit coupling,⁵ and the lower panel shows what happens if spin-rotation symmetry is broken. The numerical data follows closely the analytical prediction (7) of RMT. In particular the enhanced density of states in the presence of spin-orbit coupling is clearly seen. The first oscillations in the density of states are also captured in the dynamical model. The frequency doubling due to the reduced degeneracy ($s = 2 \rightarrow s = 1$) is apparent.

V. CONCLUSION

In conclusion, we have introduced a quantum map for the dynamics of a chaotic quantum dot with spin-orbit coupling connected to a superconductor. We have demonstrated three effects of spin-orbit coupling on the excitation spectrum of this Andreev billiard: The nar-

rowing of the distribution of the excitation gap and the appearance of oscillations in the density of states in the absence of a magnetic field; and the peak in the density of states at the Fermi level in strong magnetic field. Our numerical simulations confirm the predictions of random-matrix theory. The third effect is particularly interesting from an experimental point of view. In view of the possibility to tune the strength of spin-orbit coupling in quantum dots,^{21,22} one can imagine tuning the density of states at the Fermi level from zero to a value of twice the normal density of states.

ACKNOWLEDGMENTS

Discussions and correspondence with J. Cserti, M. C. Goorden, P. Jacquod, and J. Tworzydło are gratefully acknowledged. This work was supported by the Dutch Science Foundation NWO/FOM. We acknowledge support by the European Community's Marie Curie Research Training Network under contract MRTN-CT-2003-504574, Fundamentals of Nanoelectronics.

-
- ¹ C. W. J. Beenakker, *Lect. Notes Phys.* **667**, 131 (2005).
² A. Altland and M. R. Zirnbauer, *Phys. Rev. Lett.* **76**, 3420 (1996).
³ K. M. Frahm, P. W. Brouwer, J. A. Melsen, and C. W. J. Beenakker, *Phys. Rev. Lett.* **76**, 2981 (1996).
⁴ J. A. Melsen, P. W. Brouwer, K. M. Frahm, and C. W. J. Beenakker, *Physica Scripta* **T69**, 223 (1997).
⁵ M. C. Goorden, P. Jacquod, and C. W. J. Beenakker, *Phys. Rev. B* **72**, 064526 (2005).
⁶ A. Altland and M. R. Zirnbauer, *Phys. Rev. B* **55**, 1142 (1997).
⁷ N. M. Chtchelkatchev and Y. V. Nazarov, *Phys. Rev. Lett.* **90**, 226806 (2003).
⁸ O. V. Dimitrova and M. V. Feigel'man, *JETP* **102**, 652 (2006).
⁹ C. A. Tracy and H. Widom, *Commun. Math. Phys.* **177**, 727 (1996).
¹⁰ M. G. Vavilov, P. W. Brouwer, V. Ambegaokar, and C. W. J. Beenakker, *Phys. Rev. Lett.* **86**, 874 (2001).
¹¹ J. A. Melsen, P. W. Brouwer, K. M. Frahm, and C. W. J. Beenakker, *Europhys. Lett.* **35**, 7 (1996).
¹² A. Edelman and P.-O. Persson, *math-ph/0501068*.
¹³ P. J. Forrester, T. Nagao, and G. Honner, *Nucl. Phys. B* **553**, 601 (1999).
¹⁴ C. A. Tracy and H. Widom, *Ann. Inst. Fourier (Grenoble)* **55**, 2197 (2005).
¹⁵ P. Jacquod, H. Schomerus, and C. W. J. Beenakker, *Phys. Rev. Lett.* **90**, 207004 (2003).
¹⁶ R. Scharf, *J. Phys. A* **22**, 4223 (1989).
¹⁷ J. H. Bardarson, J. Tworzydło, and C. W. J. Beenakker, *Phys. Rev. B* **72**, 235305 (2005).
¹⁸ P. G. de Gennes, *Superconductivity of Metals and Alloys* (Benjamin, New York, 1966).
¹⁹ A. Kormanyos, Z. Kaufmann, C. J. Lambert, and J. Cserti, *Phys. Rev. B* **70**, 052512 (2004).
²⁰ Ref. 15 reported good agreement for the $\beta = 1$ gap distribution between RMT and the Andreev kicked rotator — without any need to fit E_{gap} and Δ_{gap} . We now believe that this good agreement was fortuitous, and that some 5–10% variation of these parameters is generally needed for a good agreement.
²¹ D. M. Zumbühl, J. B. Miller, C. M. Marcus, K. Campman, and A. C. Gossard, *Phys. Rev. Lett.* **89**, 276803 (2002).
²² J. B. Miller, D. M. Zumbühl, C. M. Marcus, Y. B. Lyanda-Geller, D. Goldhaber-Gordon, K. Campman, and A. C. Gossard, *Phys. Rev. Lett.* **90**, 076807 (2003).